analytical chemistry

pubs.acs.org/ac Article

Ultrasensitive Homogeneous Electrochemiluminescence Biosensor for a Transcription Factor Based on Target-Modulated Proximity Hybridization and Exonuclease III-Powered Recycling Amplification

Dan Li, Ya Li, Fang Luo,* Bin Qiu, and Zhenyu Lin*

Cite This: *Anal. Chem.* 2020, 92, 12686−12692 Read Online

ACCESS | Metrics & More | Article Recommendations

ABSTRACT: Herein an ultrasensitive homogeneous ECL biosensor has been developed for TF NF-κB p50 through target-modulated proximity hybridization coupling with exonuclease III (Exo III)-powered recycling amplification. The ECL reagent ($Ru(bpy)_3^{2+}$)-labeled hairpin DNA (HP-Rul) contains many negatively charged phosphates on the DNA chain, which cannot diffuse easily toward the negatively charged ITO electrode surface because of the large electrostatic repulsion. So a weak ECL signal can be detected. A proximity complex containing partial double strand DNA (dsDNA, as the binding site) and two hanging single-stranded DNA (ssDNA) fragments has been designed. The binding of NF-κB p50 to dsDNA effectively protects the proximity complex from digestion, forming a stable TF−DNA complex. ssDNA hybridizes with HP-Rul through proximity hybridization and hence forms a T-shape structure. This structure can be recognized by Exo III, thereby initiating the digestion process and results in the release of $Ru(bpy)_3^{2+}$-labeled mononucleotide fragments (MFs-Rul). Meanwhile, another HP-Rul is opened and hence triggers the next cycle of hybridization and digestion process; thus, multiple MFs-Rul are generated. MFs-Rul diffuse easily to the ITO electrode because of small electrostatic repulsion, resulting in an evident signal enhancement. Under the optimal conditions, the ΔECL has a linear relationship with the logarithm of NF-κB p50 concentration ranging from 0.1 to 500 pM. The detection limit is 29 fM (S/N = 3). The sensing platform has been successfully applied to detect NF-κB p50 in cell lysates and also demonstrated to work well for NF-κB p50 inhibitor detection, exhibiting great potential in the diagnosis of disease and drug discovery.

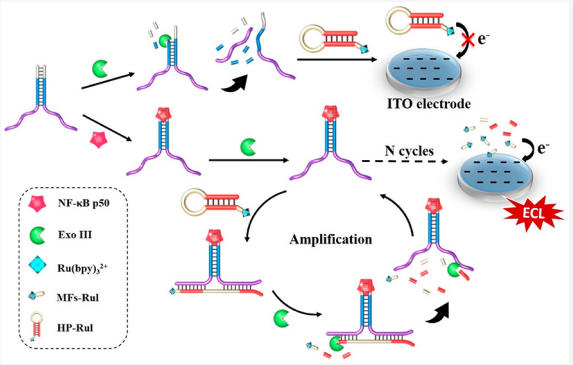

Transcription factors (TFs) can bind to specific double-stranded DNA (dsDNA) sequences and play important roles in the control of transcription of the target gene.[1] The undesired activation or inhibition of TFs may cause several diseases, including developmental disorders, autoimmune diseases, inflammation, and cancer.[2,3] Therefore, it is necessary to develop some simple and sensitive methods for TF detection. Conventional methods, such as Western blotting,[4] DNA footprinting,[5] electrophoretic mobility shift assay,[6] and enzyme-linked immunosorbent assay,[7] have been applied for TF assays. The procedures for most of these methods are cumbersome and time-consuming or involve the use of expensive antibodies or radioisotopes, thereby limiting their extensive applications. Alternatively, a variety of new technologies have been developed for TF detection, such as immunoassay,[8,9] surface-enhanced Raman scattering,[10−12] colorimetric assay,[13,14] fluorescent assay,[15−17] and electrochemical techniques.[18−23] Electrochemiluminescence (ECL) detection technology combines the advantages of high sensitivity of chemiluminescence and the flexibility of electrochemistry, and it has been employed for the detection of TFs.[24] In this detection, the DNA probe needs to be immobilized on the electrode first through a tedious process. Second, the interaction between the target and probe occurs at the interface of electrode−solution, but low efficiency occurs because of steric hindrance from the electrode surface.

DNA contains negative charges due to the negatively charged phosphates on the skeleton of DNA.[25] Different electrochemical signals can be recorded based on the discrimination of diffusion of electroactive reporter-labeled long and short DNA strands toward the negatively charged electrode surface. Hsing's group first utilized this characteristic to construct a homogeneous electrochemical biosensor for

Received: July 20, 2020
Accepted: August 10, 2020
Published: August 10, 2020

https://dx.doi.org/10.1021/acs.analchem.0c03086
Anal. Chem. 2020, 92, 12686−12692

Scheme 1. Homogeneous ECL Biosensor for NF-κB p50 Assay by Using Target-Modulated Proximity Hybridization and Exo III-Powered Signal Amplification Strategy

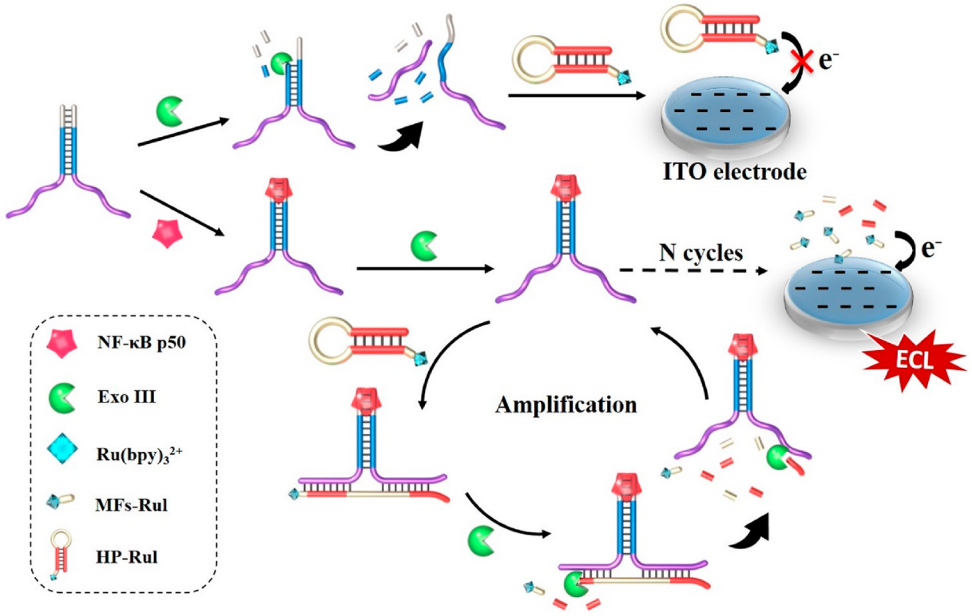

nucleic acids.[26] Afterward, more homogeneous electrochemical biosensors have been developed for diverse targets including TFs.[27−32] Our group has extended this approach to develop some homogeneous ECL biosensors for RNase A activity, the folate receptor, and ochratoxin A.[33−35] These sensors combine the advantages of ECL detection and the convenience and high efficiency of homogeneous detection.

Exonuclease III (Exo III) has been frequently applied to develop sensitive biosensors, as its usage can realize signal amplification easily.[36,37] Early reports indicated that TFs can bind with their specific DNA sequence and hence form a stable DNA−TF complex, which can prevent dsDNA digestion by Exo III.[38] The proximity hybridization assay (PHA) was first proposed by Landegren in 2002 and has been widely used in protein analysis through converting the protein-recognition process into DNA detection.[39,40] The PHA as a powerful tool is expected to be employed in constructing biosensors with high specificity and sensitivity.

In this study, an ultrasensitive homogeneous ECL biosensor has been designed for NF-κB p50 assay based on target-modulated proximity hybridization and Exo III-powered recycling amplification. The detailed principle is shown in Scheme 1. A DNA complex (called proximity complex) with partial dsDNA and two hanging ssDNA fragments was formed through partial hybridization of DNA1 with DNA2, and the dsDNA domain contains target protein recognition sequences. Target protein (NF-κB p50) can bind to its recognition site with high efficiency and hence forms a stable TF−DNA complex, which protects the proximity complex from Exo III digestion. The dsDNA domain in the excess proximity complex can be digested by Exo III completely. Subsequently, hairpin DNA labeled with $Ru(bpy)_3^{2+}$ (HP-Rul) was added. Notably, HP-Rul was delicately designed to contain a 3′-protruding terminus, which can effectively antagonize the Exo III digestion. The hanging ssDNA fragments in the TF−DNA complex hybridized with HP-Rul to form a T-shaped structure, which includes a 3′-blunt terminus and can be digested by Exo III. This resulted in the liberation of the TF−DNA complex and could be used to open another HP-Rul to trigger the next cycle of hybridization and digestion process but also released considerable $Ru(bpy)_3^{2+}$-labeled mononucleotide fragments (MFs-Rul). MFs-Rul containing a few negative charges could diffuse to the negatively charged ITO electrode easily, and an obvious ECL signal was detected. Without NF-κB p50, the dsDNA domain in the proximity complex was digested and resulted in the dissociation of two ssDNA fragments, as the estimated melting temperatures (T_m) of these fragments and HP-Rul are designed to be lower than the reaction temperature and make it unable to open the HP-Rul. Nearly no MFs-Rul were generated. Meanwhile, the intact HP-Rul contained relatively large negative charges on the backbone of DNA, hindering it close to the negatively charged ITO electrode because of the strong electrostatic repulsion, and a negligible ECL signal was obtained. The enhanced ECL signal has some relationship with the concentration of NF-κB p50. By these means, an ultrasensitive homogeneous ECL biosensor for NF-κB p50 can be developed.

EXPERIMENTAL SECTION

Reagent and Materials. Exo III (containing 10× Exo III reaction buffer) was bought from Thermo Fisher Scientific (Shanghai, China). The purified human recombinant NF-κB p50 was provided by Cayman Chemical (Ann Arbor, MI). Tripropylamine (TPrA), ruthenium(II) ($Ru(bpy)_3Cl_2$), carcinoembryonic antigen (CEA), human serum albumin (HSA), alpha fetoprotein (AFP), and squamous cell carcinoma antigen (SCCA) were obtained from Sigma-Aldrich (St. Louis, MO). Oridonin was bought from Solarbio (Beijing, China). Ultrapure water (Milli-Q, Millipore, resistance 18.2 MΩ cm) was used throughout the experiments. HPLC-purified oligonucleotides were purchased from Sangon Biotech Co., Ltd. (Shanghai, China). The sequences were displayed in following.

DNA1: ATCGGGACTTTAGGTGAGGTC-AACAGGTCA
DNA2: CAGCTTACACTGGAAATCCCGAT
HP: GGTCATCGGTTTGACTAGCTG

https://dx.doi.org/10.1021/acs.analchem.0c03086
Anal. Chem. 2020, 92, 12686−12692

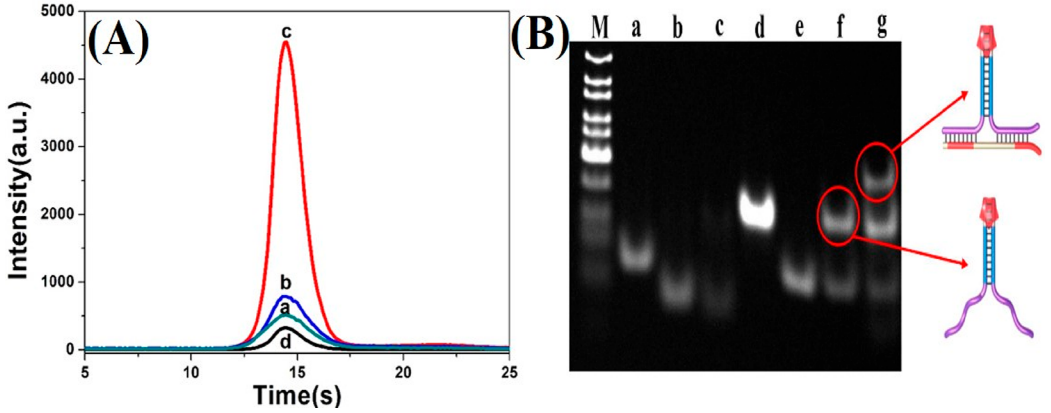

Figure 1. (A) ECL responses under different conditions. (a) HP-Rul; (b) proximity complex + Exo III + HP-Rul; (c) proximity complex + NF-κB p50 + Exo III + HP-Rul; (d) proximity complex + NF-κB p50 + HP-Rul. The concentrations of proximity complex, NF-κB p50, HP-Rul, and Exo III were 0.5 μM, 5.0 pM, 1.0 μM, and 0.2 U μL^{-1}, respectively. Conditions: TPrA concentration: 0.02 M; CV scanning potential range: 0.6 to 1.6 V; scanning rate: 100 mV/s. (B) PAGE analysis of the products of the reaction system. Lane M: DNA marker; lane a: DNA1; lane b: DNA2; lane c: HP; lane d: DNA1/DNA2 duplex (proximity complex); lane e: proximity complex + Exo III; lane f: proximity complex + NF-κB p50 + Exo III; lane g: proximity complex + NF-κB p50 + Exo III + HP (Exo III was inactive before adding HP). The concentrations of all DNA sequences were 1.0 μM, the concentration of NF-κB p50 was settled as 50 pM, and Exo III concentration was 0.2 U μL^{-1}.

The HP-Rul was prepared according to previously reported procedures.[32] Buffer solution used in the work as follows:

Tris-HCl buffer: 10 mM Tris, 100 mM NaCl, pH 7.5.

Reaction buffer: 10 mM Tris, 2 mM $MgCl_2$,100 mM KCl, 0.25 mM DTT, 0.1 mM EDTA, pH 7.5.

Binding buffer: 10 mM Tris, 2 mM $MgCl_2$,100 mM KCl, 0.25 mM DTT, 0.1 mM EDTA, 0.1 mg/mL yeast tRNA, pH 7.5.

Apparatus. The ECL signals were measured by a lab-built ECL detection system. A CHI660E electrochemical workstation (Chenhua Instruments, Shanghai, China) was used to control the potential scanning, and a BPCL ultraweak luminescence analyzer (Institute of Biophysics, Chinese Academy of Science, Beijing, China) was used to collect the ECL signal. A three-electrode electrochemical system contains a pretreated ITO working electrode (the working area was 5 mm × 3 mm, obtained from Huanan Xiangcheng, Shenzhen, China, resistance ≤6Ω), a Ag/AgCl reference electrode saturated with KCl, and a counter electrode made from platinum wires. The voltage of the photomultiplier tube (PMT) of BPCL analyzer was settled as −900 V.

Before using, the ITO working electrode was sonicated in an alconox solution (2 g of alconox was dissolved in 100 mL of ultrapure water), 2-propanol, and ultrapure water for 15 min, in order. By this simple procedure, the ITO electrode surface can be negatively charged.

Exo III-Powered Homogeneous ECL Detection. The ssDNA DNA1 (20 μM) and DNA2 (20 μM) were mixed with the volume ratio of 1:1 and denatured at 95 °C for 5 min first. Then the mixed solution was cooled gradually to room temperature to form a proximity complex which contains partial dsDNA domain and two hanging ssDNA fragments. The prepared solution was kept at 4 °C prior to use. For NF-κB p50 detection, 0.5 μM proximity complex was mixed with various concentrations of NF-κB p50 in binding buffer (20 μL) and incubated for 30 min under room temperature to enable target binding to its recognition sites. Then Exo III (0.2 U μL^{-1}) was added to the system and incubated at 37 °C for 1.5 h to digest the redundant proximity complex completely. Subsequently, 1.0 μM HP-Rul and a certain amount of the reaction buffer were added to obtain a total volume of 50 μL and then incubated at 37 °C for a certain period of time to realize the Exo III-powered cycling. The control assay was conducted under the same condition without adding NF-κB p50. ECL detections were carried out in the resulting solution containing 0.02 M TPrA under cyclic voltammetry scanning in the range of 0.6−1.6 V and with a scan rate of 100 mV/s. Each sample was detected five times, and the averaged value was used for quantification.

Gel Electrophoresis. 12% Polyacrylamide gel electrophoresis (PAGE) was conducted to verify the binding of NF-κB p50 with the proximity complex and the formation of the hybrid product in the proposed biosensor. In the gel electrophoresis assay, HP-Rul was displaced by the nonlabeled hairpin DNA with the same sequence (HP) to circumvent the effect of $Ru(bpy)_3^{2+}$. The project was performed in 0.5× Tris-borate-EDTA (TBE) buffer (pH 8.4) at a constant voltage of 80 V for 2.5 h at room temperature. The obtained gel was imaged by a gel imaging system.

Detection of NF-κB p50 in Cell Lysate. Briefly, 0.5 μM proximity complex and 5 μL of MCF-7 cell lysate (1.0×10^6 cells/mL) were incubated in binding buffer (20 μL). The cell lysate was 10-fold diluted to a final volume was 50 μL. The other procedures were the same as mentioned above.

RESULTS AND DISCUSSION

Feasibility Assay. Comparative assays were initially carried to verify the feasibility of the proposed system. HP-Rul contains a large amount of negatively charged phosphates on the DNA chain, and the ITO electrode contains a negative charge as well after pretreatment. The electrostatic repulsion prevented HP-Rul from reaching the electrode surface, so a negligible ECL signal was detected when just HP-Rul was added to the system (curve a in Figure 1(A)). Similarly, only a weak ECL signal was recorded after adding proximity complex, Exo III, and HP-Rul to the system (curve b), demonstrating that the dsDNA domain in the proximity complex is digested by Exo III, and the product could not initiate HP-Rul and enzyme digestion afterward. The weak ECL signal might be attributed to nonspecific digestion of Exo III toward HP-Rul.

https://dx.doi.org/10.1021/acs.analchem.0c03086
Anal. Chem. 2020, 92, 12686−12692

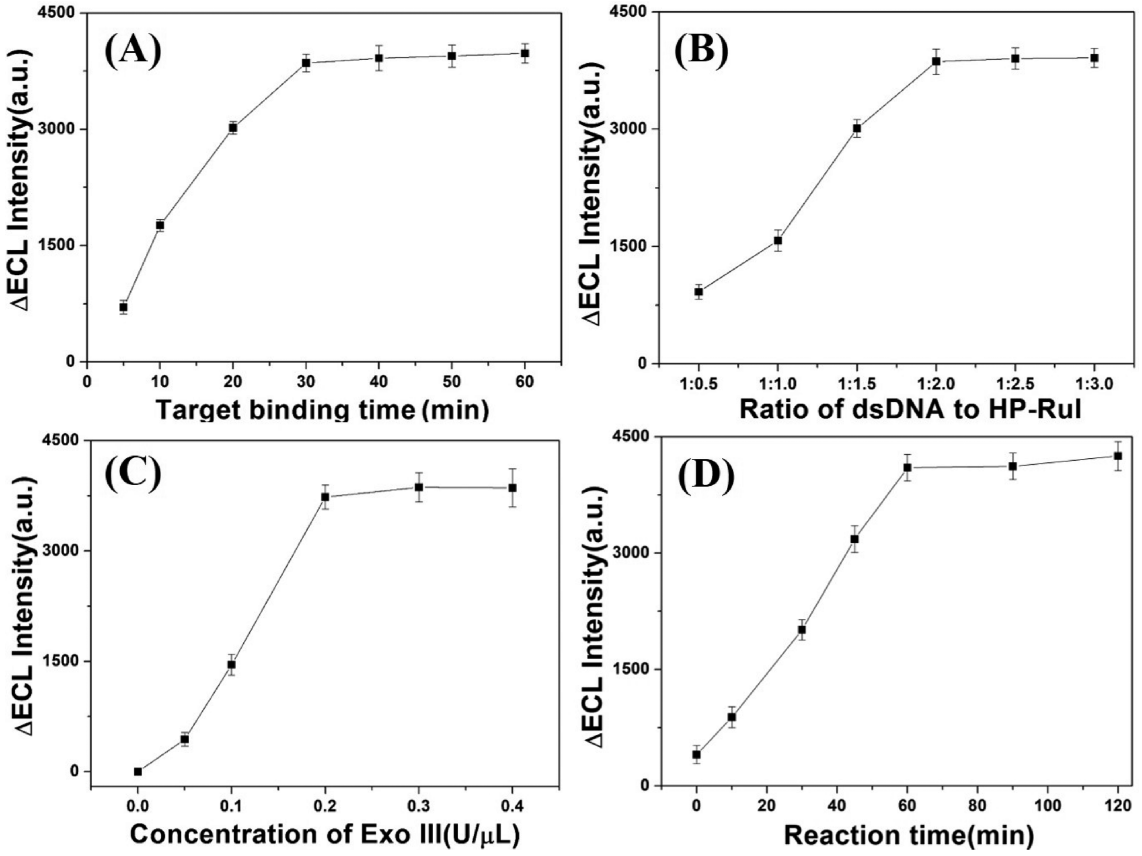

Figure 2. Effect of the (A) binding time of target and proximity complex; (B) the concentration ratio of the proximity complex and HP-Rul; (C) concentration of Exo III and (D) digestion time of Exo III on ECL signal detected. The concentration of NF-κB p50 was 5.0 pM. Error bars represent the standard deviation of five repetitive measurements. The other conditions are the same as those in Figure 1(A).

When the proximity complex was incubated with NF-κB p50 before adding Exo III and HP-Rul, the ECL signal was significantly increased (curve c), indicating that the formation of the DNA−TF complex severely hinders the digestion of Exo III, and thus ssDNA fragments of the preserved proximity complex can be used to open up HP-Rul. Then the Exo III digestion is performed, and the DNA−TF complex is released and hence unfolds another HP-Rul to trigger the next cycle of Exo III recycling amplification reaction. As a result, multiple HP-Rul with a fewer negative charges are produced and therefore leads to the enhanced ECL signal. However, if only NF-κB p50 but no Exo III was added, a significantly reduced ECL signal was detected (curve d). This phenomenon indicates that no signal amplification occurs without the presence of Exo III.

A gel electrophoresis assay was employed to test the mechanism of the designed system as well. As shown in Figure 1(B), DNA1 (lane a), DNA2 (lane b), and HP (lane c) were used as reference bands. There was a bright stripe of the proximity complex formed by partial hybridization of DNA1 and DNA2 (lane d). Only a DNA1 band was obtained when the proximity complex was incubated with Exo III, demonstrating that the dsDNA domain is completely digested by Exo III (lane e). As expected, a portion of the dsDNA strip was retained after the addition of target NF-κB p50, because NF-κB p50 can bind with its recognition DNA sites and hence forms a stable TF−DNA complex, which can effectively resist the Exo III digestion (lane f). A new higher band was obvious when HP was added further to the system, indicating that HP was consumed to form a new structure (lane g). All the above outcomes confirmed that the sensing platform for highly specific NF-κB p50 assay was successfully constructed.

Optimization of Experimental Conditions. Various experimental conditions were first optimized to reach the best sensing performance of the system. The effect of binding time of NF-κB p50 with the proximity complex was investigated first. As shown in Figure 2(A), the ΔECL (the difference in ECL signal detected in the presence and absence of NF-κB p50) was enhanced gradually with prolonged binding time and then tended to reach a plateau after 30 min. Thus, this time was chosen as the optimized binding time for the subsequent study.

HP-Rul concentration plays an important role in the biosensor. A low concentration of HP-Rul could not support sufficient signal amplification cycles, whereas excessive HP-Rul would lead to a high background signal. Therefore, we subsequently optimized the ratio of proximity complex and HP-Rul. The concentration of the proximity complex was fixed, and then the optimum HP-Rul concentration was obtained through testing the concentration ratios of the proximity complex to HP-Rul. As displayed in Figure 2(B), the ΔECL increased with the increase in ratio and finally reached a steady value at a ratio of 1:2, which was used as the optimal ratio of dsDNA to HP-Rul in this work.

The influences of Exo III concentration and amplification time after the addition of Exo III were investigated, as they were the key factors influencing the cycling amplification efficiency. ΔECL increased with the enhancement of Exo III

https://dx.doi.org/10.1021/acs.analchem.0c03086
Anal. Chem. 2020, 92, 12686−12692

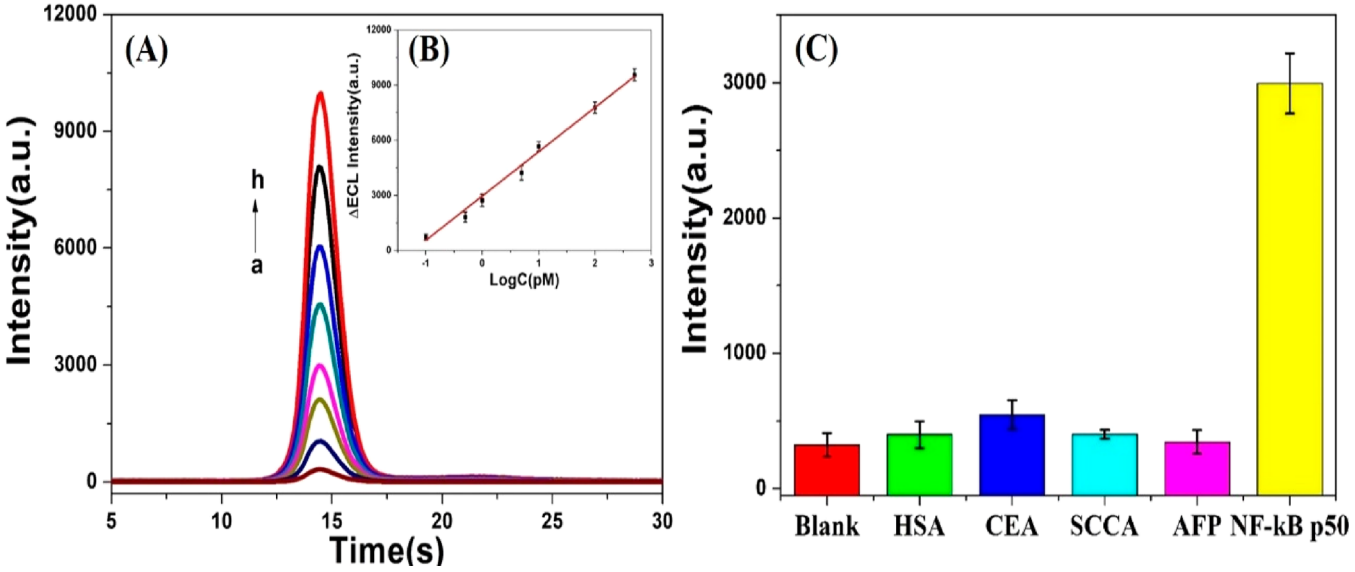

Figure 3. (A) ECL responses of the reaction system in the presence of NF-κB p50 at different concentrations. From a to h: 0, 0.1, 0.5 pM, 1.0, 5.0, 10.0, 100, 500 pM. (B) The linear relationship between the enhanced ECL intensity and the logarithm of NF-κB p50 concentration. (C) Selectivity of the proposed biosensor to NF-κB p50 by comparing the ECL response of the reaction system in the presence of NF-κB p50 (1.0 pM) to some typical interfering proteins, including HSA (100 pM), CEA (100 pM), AFP (100 pM), SCCA (100 pM), and the blank. The other conditions are the same as that in Figure 1(A).

concentration first and did not increase greatly after 0.2 U μL^{-1} (shown in Figure 2(C)), so 0.2 U μL^{-1} was hence chosen for the following assays. In addition, the ΔECL increased gradually as time went on first and reached a plateau after 60 min (Figure 2(D)), which was thus selected as the optimal amplification time for this work.

Performance of the Developed ECL Biosensor. Under the optimal conditions, the performance of the sensing system was evaluated by adding various concentrations of NF-κB p50 to the reaction system. Figure 3(A) indicates that the ECL signal of the system increased with the increase of NF-κB p50 concentration. ΔECL has a good linear relationship with the logarithm of NF-κB p50 concentration in the range of 0.1 pM to 500 pM (Figure 3(B)). The linear regression equation is

$$\Delta ECL/counts = 2963 + 2049 \log C/pM \quad (1)$$

where C is the concentration of NF-κB p50. The correlation coefficient is 0.9918. The limit of detection (LOD) is 29 fM (S/N = 3). The LODs of early reported ECL detection and homogeneous electrochemical detection are 3.2 pM[24] and 10 pM,[30] respectively. The LOD of the proposed method is lower than that in previously reported methods for NF-κB p50 detection.[17,20,24,30,41,42] The high sensitivity can be attributed to the excellent target-induced proximity hybridization as well as the powerful Exo III-assisted signal amplification and high sensitivity of ECL detection.

The selectivity of the proposed biosensor was validated by comparing the ECL response to some typical interference proteins, including HSA, CEA, AFP and SCCA. The concentrations of interferents are 100-fold higher than the target concentration. As illustrated in Figure 3(C), a remarkable ECL signal was observed only when the target was added, whereas no obvious ECL signals enhancements were obtained when the reaction system was incubated with these interfering substances. Considering the above results, it can be concluded that this biosensor possesses high selectivity toward NF-κB p50. The reproducibility of the proposed ECL sensor was tested also, and the relative standard deviation (RSD) was 4.6% (n = 5) at the target concentration of 50 pM. This indicated that the ECL biosensor for NF-κB p50 has good reproducibility.

Detection of Endogenous NF-κB p50 and Inhibitor. The real application of the proposed method to detect endogenous NF-κB p50 was investigated. The NF-κB p50 in the cell lysates of MCF-7 cell lines was detected to be 56.5 pM. Then the standard addition recovery rate was tested to verify the validity of the proposed method. As shown in Table 1, the standard addition recovery rates were in the range of 97.3−103.6% and the RSD was in the range of 3.8−4.7%. Therefore, the proposed strategy exhibits excellent precision and accuracy for NF-κB p50 detection and has great potential to be applied in clinical tests.

Table 1. Results of NF-κB p50 Detection in 10% (v/v) MCF-7 Cell Lysate (n = 5)

samples	NF-κB p50 added (pM)	total found (pM)	recovery (%)	RSD (%)
1	0	56.5	–	4.1
2	30	85.7	97.3	4.7
3	60	115.3	98.0	4.2
4	100	158.2	101.7	4.3
5	200	263.7	103.6	3.8

Facile evaluation of the inhibitory capability of compounds against NF-κB p50 will greatly assist drug development for diseases related to NF-κB p50. Oridonin can retard the binding between NF-κB p50 and corresponding recognition sites in the proximity complex and was chosen as a model inhibitor in this study to demonstrate the possibility of the proposed homogeneous ECL technique for inhibitor detection. After the addition of oridonin (0.02 μM), a reduced ECL signal was obtained as compared with that without oridonin. And ECL signal was further decreased when increasing the oridonin concentration (0.2 μM). There is a relationship between ECL

https://dx.doi.org/10.1021/acs.analchem.0c03086
Anal. Chem. 2020, 92, 12686−12692

intensity and oridonin concentration (data are not shown). These results confirm that oridonin is an effective NF-κB p50 activity inhibitor and highlight that the proposed method can be used to detect the inhibitor concentration.

CONCLUSION

In summary, taking advantage of the different electrostatic repulsions between different length DNAs toward the negatively charged ITO electrode, an ultrasensitive homogeneous ECL biosensor for NF-κB p50 has been successfully constructed. The sensor avoids tedious procedures of DNA probe modification on the electrode. The interaction between target and DNA occurs in homogeneous solution instead of at the electrode−solution interface and has high reaction efficiency. This method exhibits superb sensitive and selective behavior toward NF-κB p50 detection, which can be attributed to the powerful Exo III-assisted signal amplification, high sensitivity of ECL detection technology, and the excellent specificity of NF-κB p50 for its recognition sites. The applications of the developed ECL biosensor for NF-κB p50 assay in diluted cell lysates and even in the detection of NF-κB p50 activity inhibition have been achieved with satisfactory results. Taken together, the proposed homogeneous ECL method not only offers a promising strategy for reliable quantification of NF-κB p50 but also has great potential for NF-κB p50-related biomedical research.

AUTHOR INFORMATION

Corresponding Authors

Fang Luo − *Ministry of Education Key Laboratory for Analytical Science of Food Safety and Biology, Fujian Provincial Key Laboratory of Analysis and Detection for Food Safety, College of Chemistry and College of Biological Science and Engineering, Fuzhou University, Fuzhou, Fujian 350116, China*; Email: luofang@fzu.edu.cn

Zhenyu Lin − *Ministry of Education Key Laboratory for Analytical Science of Food Safety and Biology, Fujian Provincial Key Laboratory of Analysis and Detection for Food Safety, College of Chemistry, Fuzhou University, Fuzhou, Fujian 350116, China*; orcid.org/0000-0001-7890-6812; Email: zylin@fzu.edu.cn

Authors

Dan Li − *Ministry of Education Key Laboratory for Analytical Science of Food Safety and Biology, Fujian Provincial Key Laboratory of Analysis and Detection for Food Safety, College of Chemistry, Fuzhou University, Fuzhou, Fujian 350116, China*

Ya Li − *Department of Ultrasound, Fourth People's Hospital of Taizhou City, Jianshu 225300, China*

Bin Qiu − *Ministry of Education Key Laboratory for Analytical Science of Food Safety and Biology, Fujian Provincial Key Laboratory of Analysis and Detection for Food Safety, College of Chemistry, Fuzhou University, Fuzhou, Fujian 350116, China*

Complete contact information is available at: https://pubs.acs.org/10.1021/acs.analchem.0c03086

Notes

The authors declare no competing financial interest.

ACKNOWLEDGMENTS

This project was financially supported by National Sciences Foundation of China (no. 21775026, 21904020, 21974020), the cooperative project of production and study in University of Fujian Province (2018Y4007), the Sciences Foundation of Fujian Province (2018J01685, 2018J01682).

REFERENCES

(1) Papavassiliou, A. G. *N. Engl. J. Med.* **1995**, *332*, 45−47.
(2) Darnell, J. E., Jr. *Nat. Rev. Cancer* **2002**, *2*, 740.
(3) Libermann, T. A.; Zerbini, L. F. *Curr. Gene Ther.* **2006**, *6*, 17−33.
(4) Bowen, B.; Steinberg, J.; Laemmli, U. K.; Weintraub, H. *Nucleic Acids Res.* **1980**, *8*, 1−20.
(5) Hampshire, A. J.; Rusling, D. A.; Broughton-Head, V. J.; Fox, K. R. *Methods* **2007**, *42*, 128−140.
(6) Garner, M. M.; Revzin, A. *Nucleic Acids Res.* **1981**, *9*, 3047−3060.
(7) Renard, P.; Ernest, I.; Houbion, A.; Art, M.; Le Calvez, H.; Raes, M.; Remacle, J. *Nucleic Acids Res.* **2001**, *29*, E21.
(8) Gupta, S. V.; McGowen, R. M.; Callewaert, D. M.; Brown, T. R.; Li, Y. W.; Sarkar, F. H. *J. Immunoassay Immunochem.* **2005**, *26*, 125−143.
(9) Wang, J.; Li, M. L.; Hua, D.; Chen, Q. *BioTechniques* **2006**, *41*, 79−89.
(10) Bonham, A. J.; Braun, G.; Pavel, I.; Moskovits, M.; Reich, N. O. *J. Am. Chem. Soc.* **2007**, *129*, 14572−14573.
(11) Schutz, M.; Steinigeweg, D.; Salehi, M.; Kompe, K.; Schlucker, S. *Chem. Commun.* **2011**, *47*, 4216−4218.
(12) Bizzarri, A. R.; Moscetti, I.; Cannistraro, S. *Anal. Chim. Acta* **2018**, *1029*, 86−96.
(13) Ou, L. J.; Jin, P. Y.; Chu, X.; Jiang, J. H.; Yu, R. Q. *Anal. Chem.* **2010**, *82*, 6015−6024.
(14) Zhang, Y.; Hu, J.; Zhang, C. Y. *Anal. Chem.* **2012**, *84*, 9544−9549.
(15) Vallee-Belisle, A.; Bonham, A. J.; Reich, N. O.; Ricci, F.; Plaxco, K. W. *J. Am. Chem. Soc.* **2011**, *133*, 13836−13839.
(16) Zhu, D.; Wang, L.; Xu, X.; Jiang, W. *Biosens. Bioelectron.* **2017**, *89*, 978−983.
(17) Li, B.; Xu, L.; Chen, Y.; Zhu, W.; Shen, X.; Zhu, C.; Luo, J.; Li, X.; Hong, J.; Zhou, X. *Anal. Chem.* **2017**, *89*, 7316−7323.
(18) Gorodetsky, A. A.; Ebrahim, A.; Barton, J. K. *J. Am. Chem. Soc.* **2008**, *130*, 2924−2925.
(19) Bonham, A. J.; Hsieh, K.; Ferguson, B. S.; Vallee-Belisle, A.; Ricci, F.; Soh, H. T.; Plaxco, K. W. *J. Am. Chem. Soc.* **2012**, *134*, 3346−3348.
(20) Shen, M.; Yang, M.; Li, H.; Liang, Z.; Li, G. *Electrochim. Acta* **2012**, *60*, 309−313.
(21) Chen, J. H.; Zhang, X.; Cai, S.; Wu, D.; Lin, J.; Li, C.; Zhang, J. *Biosens. Bioelectron.* **2014**, *53*, 12−17.
(22) Deng, K.; Li, C.; Huang, H.; Li, X. *Sens. Actuators, B* **2017**, *238*, 1302−1308.
(23) Yu, H.; Zhang, W.; Lv, S.; Han, J.; Xie, G.; Chen, S. *Chem. Commun.* **2018**, *54*, 11901−11904.
(24) Fan, Z. Q.; Wang, J. F.; Hao, N.; Li, Y. H.; Yin, Y. H.; Wang, Z. P.; Ding, Y. D.; Zhao, J. F.; Zhang, K.; Huang, W. *Chem. Commun.* **2019**, *55*, 11892−11895.
(25) Watson, J. D.; Crick, F. H. C. *Nature* **1953**, *171*, 737.
(26) Xuan, F.; Luo, X.; Hsing, I. M. *Biosens. Bioelectron.* **2012**, *35*, 230−234.
(27) Wang, X.; Dong, S.; Hou, T.; Liu, L.; Liu, X.; Li, F. *Analyst* **2016**, *141*, 1830−1836.
(28) Liu, X.; Li, W.; Hou, T.; Dong, S.; Yu, G.; Li, F. *Anal. Chem.* **2015**, *87*, 4030−4036.
(29) Tan, Y.; Wei, X.; Zhang, Y.; Wang, P.; Qiu, B.; Guo, L.; Lin, Z.; Yang, H. H. *Anal. Chem.* **2015**, *87*, 11826−11831.
(30) Lu, L.; Su, H.; Li, F. *Anal. Chem.* **2017**, *89*, 8328−8334.
(31) Fu, C.; Liu, C.; Li, Y.; Guo, Y.; Luo, F.; Wang, P.; Guo, L.; Qiu, B.; Lin, Z. *Anal. Chem.* **2016**, *88*, 10176−10182.
(32) Chang, J.; Wang, X.; Wang, J.; Li, H.; Li, F. *Anal. Chem.* **2019**, *91*, 3604−3610.

(33) Ni, J. C.; Lin, H.; Yang, W. Q.; Liao, Y. H.; Wang, Q. X.; Luo, F.; Guo, L. H.; Qiu, B.; Lin, Z. Y. *Anal. Chem.* **2019**, *91*, 14751−14756.
(34) Ni, J. C.; Wang, Q. X.; Yang, W. Q.; Zhao, M. M.; Zhang, Y.; Guo, L. H.; Qiu, B.; Lin, Z. Y.; Yang, H. H. *Biosens. Bioelectron.* **2016**, *86*, 496−501.
(35) Ni, J. C.; Yang, W. Q.; Wang, Q. X.; Luo, F.; Guo, L. H.; Qiu, B.; Lin, Z. Y.; Yang, H. H. *Biosens. Bioelectron.* **2018**, *105*, 182−187.
(36) Zuo, X. L.; Xia, F.; Xiao, Y.; Plaxco, K. W. *J. Am. Chem. Soc.* **2010**, *132*, 1816−1818.
(37) Huang, K. J.; Shuai, H. L.; Zhang, J. Z. *Biosens. Bioelectron.* **2016**, *77*, 69−75.
(38) Xu, X.; Zhao, Z.; Qin, L.; Wei, W.; Levine, J. E.; Mirkin, C. A. *Anal. Chem.* **2008**, *80*, 5616−5621.
(39) Fredriksson, S.; Gullberg, M.; Jarvius, J.; Olsson, C.; Pietras, K.; Gústafsdóttir, S. M.; Östman, A.; Landegren, U. *Nat. Biotechnol.* **2002**, *20*, 473−447.
(40) Wang, X.; Gao, H.; Qi, H.; Gao, Q.; Zhang, C. *Anal. Chem.* **2018**, *90*, 3013−3018.
(41) Ma, D. L.; Xu, T.; Chan, D. S.; Man, B. Y.; Fong, W. F.; Leung, C. H. *Nucleic Acids Res.* **2011**, *39*, No. e67.
(42) Liu, J. J.; Song, X. R.; Wang, Y. W.; Chen, G. N.; Yang, H. H. *Nanoscale* **2012**, *4*, 3655−3659.

https://dx.doi.org/10.1021/acs.analchem.0c03086
Anal. Chem. 2020, 92, 12686−12692